



HAL
open science

Condensation heat transfer on enhanced surface tubes: experimental results and predictive theory

Mourad Belghazi, André Bontemps, Christophe Marvillet

► To cite this version:

Mourad Belghazi, André Bontemps, Christophe Marvillet. Condensation heat transfer on enhanced surface tubes: experimental results and predictive theory. *Journal of Heat Transfer*, 2002, 124, pp.754-760. 10.1115/1.1459728 . hal-00184114

HAL Id: hal-00184114

<https://hal.science/hal-00184114>

Submitted on 11 Feb 2020

HAL is a multi-disciplinary open access archive for the deposit and dissemination of scientific research documents, whether they are published or not. The documents may come from teaching and research institutions in France or abroad, or from public or private research centers.

L'archive ouverte pluridisciplinaire **HAL**, est destinée au dépôt et à la diffusion de documents scientifiques de niveau recherche, publiés ou non, émanant des établissements d'enseignement et de recherche français ou étrangers, des laboratoires publics ou privés.



Distributed under a Creative Commons Attribution 4.0 International License

Condensation Heat Transfer on Enhanced Surface Tubes: Experimental Results and Predictive Theory

Condensation heat transfer in a bundle of horizontal enhanced surface copper tubes (Gewa C+ tubes) has been experimentally investigated, and a comparison with trapezoidal shaped fin tubes with several fin spacing has been made. These tubes have a specific surface three-dimensional geometry (notched fins) and the fluids used are either pure refrigerant (HFC134a) or binary mixtures of refrigerants (HFC23/HFC134a). For the pure fluid and a Gewa C+ single tube, the results were analyzed with a specifically developed model, taking into account both gravity and surface tension effects. For the bundle and for a pure fluid, the inundation of the lowest tubes has a strong effect on the Gewa C+ tube performances contrary to the finned tubes. For the mixture, the heat transfer coefficient decreases dramatically for the Gewa C+ tube.

Keywords: Bundles, Condensation, Finned Surfaces, Zeotropic Mixture, Horizontal Tubes

Introduction

A large number of specifically designed enhanced surface tubes have been tested to find the best surface geometry for condensing either pure fluids or vapor mixtures. These surfaces can be classified according to three types: one-dimensional surfaces (smooth tubes), two-dimensional surfaces (with transverse plain fins) and three-dimensional surfaces (with interrupted fins, spines, etc . . .). Theoretical models to predict the heat transfer coefficient for single low-finned tubes with trapezoidal (or rectangular) fins have been well developed since the 1940s, in particular by the pioneering work of Beatty and Katz [1]. Their model assumed that condensate is drained via gravity only. They neglected surface tension forces, which generally have an important role at the fin tip, since they are responsible for the draining of condensate from the tip to the fin flanks, and because the major part of heat transfer occurs at the fin tip. The surface tension forces also have a non-beneficial effect due to condensate retention along the underside of the tube. Theoretical models combining both gravity and surface tension forces, are used to predict the Heat Transfer Coefficient (HTC) of a single horizontal tube with sufficient accuracy (Karkhu and Borovkov [2], Webb et al. [3], Honda and Nozu [4], Adamek and Webb [5], Rose [6], Sreepathi et al. [7]). The most simple proposed by Rose [6], is a semi-empirical model for a horizontal tube having trapezoidal fins. An enhancement ratio $\varepsilon_{\Delta T}$ is defined as the ratio of the heat transfer coefficient for a finned tube to that for a plain tube, based on plain tube area at the fin root diameter for the same ΔT ($\Delta T = T_{\text{sat}} - T_w$). To compare his model to experimental results, Rose used various finned tubes with different pitches, heights and diameters as well as various fluids (water, ethylene glycol, methanol, R113, R11, R12 . . .).

Since the work of Gregorig, [8], many theoretical studies to optimize the fin profiles of two-dimensional circumferential fins have been carried out. Adamek [9] in his theoretical approach assumed the condensate to be drained by surface tension forces only and showed that around the fin crest the best heat transfer is

given by a profile curvature depending on the path length at a power of -0.5 instead of 2.0 as proposed by Gregorig. More recently, Zhu and Honda [10] and Honda and Kim [11] have performed numerical calculations to optimize the fin profiles of two-dimensional circumferential fins.

There are other numerical approaches to optimize enhanced surfaces. Honda and Makishi [12] in a two dimensional adaptation showed that by creating a circumferential rib on a fin, the values of the HTC can be 27 to 58 percent higher than the best performing fin profile proposed in the previous studies. Further three-dimensional adaptations to extended surfaces have been carried out. The first systematic investigation was by Webb et al. [13] but does not allow a conclusive opinion to be drawn. Honda et al. [14,15] compared the heat transfer performance of several two-dimensional and three-dimensional fin geometries. Their results showed that the heat transfer performance of the best two-dimensional and those of the tested three-dimensional tubes are comparable. A specific type of three-dimensional fin was realized by Wang et al. [16] by creating radial ridges on the fin flanks. They found that the heat transfer performance was 30 to 40 percent higher than commercially available three-dimensional fin tubes.

The results obtained for a single tube cannot be extended to a tube bundle and a fin profile optimized for a single tube can be non-optimized for a tube bundle making, these models for a single tube inapplicable to tube banks, since the heat transfer in the lower rows is affected by condensate inundation and the HTC is lower for these tubes. It has been shown that, in this case, three-dimensional geometries are not favorable (Webb and Murawski [17], Honda et al. [14,15]). In the literature there are several approaches to this problem. The simplest consists of multiplication of the heat transfer for a single tube by a factor less than unity, taking into account the row position in the bundle.

In this paper, experiments were carried out to determine the HTC during condensation of R134a and a zeotropic mixture of R23 and R134a, on horizontal tubes with three-dimensional enhanced surfaces. A new type of notched fin tube (called Gewa C+ tube) has been studied and the results have been compared to those obtained for smooth tubes or integral-fin tubes with trapezoidal fins. This notched tube can be considered as a combination

M. Belghazi

Research Student,
Groupement pour la Recherche
sur les Echangeurs Thermiques
(GRETh), CEA Grenoble,
17, avenue des martyrs,
38054 Grenoble cedex 9, France

A. Bontemps

Professor,
Laboratoire des Ecoulements Géophysiques et
Industriels (LEGI/GRETh),
Université Joseph Fourier,
Grenoble, France,
CEA Grenoble, 17, avenue des martyrs, 38054
Grenoble cedex 9, France

C. Marvillet

Research Engineer,
Groupement pour la Recherche
sur les Echangeurs Thermiques
(GRETh), CEA Grenoble,
17, avenue des martyrs,
38054 Grenoble cedex 9, France

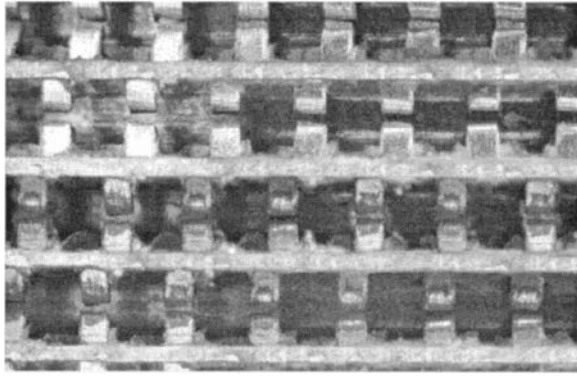


Fig. 1 Optical microscope view of a notched fin tube (Gewa C+)

of the enhanced tube with a circumferential rib (Honda and Kim [11]) with the tube having radial ridges on the fin flank (Wang et al. [16]). The notches seen in Fig. 1 can be considered as part of a rib and the space between notches as radial ridges. One can expect that such a fin geometry will be efficient in condensation heat transfer.

There are few experiments on condensation of HFC134a on low finned tubes. In the work of Blanc et al. [18] the HTC on trapezoidal fin tubes (K26) is compared with another type of finned tube as well as with current theories. Honda et al. [19] measured the row-by-row heat transfer coefficients of HFC134a condensing on a bundle of tubes having 26 fins/inch and a diameter at the fin root of 15.8 mm. Their results are slightly lower than those of Blanc et al., Cheng and Wang [20], and Agrawal et al. [21] conducted experiments on condensation of HFC134a using several types of low finned tubes. For a vertical column of three tubes with trapezoidal fins no significant inundation effect is observed [20]. The variation of the HTC in function of ΔT for a single tube was carried out by Agrawal et al. [21].

Studies covering the condensation of zeotropic mixtures are essentially confined to flat plates and smooth tubes. Hijikata and Himeno [22] conducted experiments using horizontal finned tubes during condensation of the binary mixture (90 percent R113+ 10 percent R114), and they found that the tube with high fins (3 mm) is better than the one with small fins (0.8 mm). Honda et al. [23] conducted experiments during condensation of a downward-flowing zeotropic mixture HFC123/HFC134a (about 9 percent HFC134a at the test section inlet), on a 13×15 (columns × rows) staggered bundle of horizontal low finned tubes. Their experimental data show that both the heat and the mass transfer

coefficients increased with the row number up to the third (or the second) row, then decreased monotonically with increasing row number, finally to increase at the last row.

Experimental Apparatus and Reduction of Data

The experimental apparatus consists of a thermosyphon refrigerant loop and a forced circulation coolant (water) loop (Fig. 2). The test rig used in this investigation is basically the same as that used in the previous study by Belghazi et al. [24].

In the refrigerant loop the vapor is generated in a boiler heated with hot water which is itself heated electrically. The vapor flows towards the test section, passes vertically downwards and condenses outside the water cooled tubes. The test section (Fig. 3) is a stainless steel duct and contains a staggered copper tube bank consisting of 13 rows, each of 2 (even rows) or 3 tubes (odd rows). The cross-hatched tubes are dummies (no heat exchange), while the others are active. Half tubes are attached to the vertical walls of the test section in order to eliminate vapor by-pass. A metallic rod with a diameter of 11 mm was inserted in each active tube in order to increase the water velocity. In this way the heat transfer is enhanced on the coolant side. The horizontal tube pitch is 24 mm, whereas the vertical pitch is 20 mm. The length of the tubes is 300 mm. The characteristics of the tested tubes are given in Table 1. Since the water flow rate is equally distributed in all active tubes (it is controlled by means of 13 rotameters, one on each row), it is deduced from the water flow rate in the coolant loop, measured by an electromagnetic flow meter, with an accuracy of ± 0.5 percent. The vapor velocity is less than 2 m/s and the vapor temperature inlet was maintained at 40°C. Temperatures were measured by type E thermocouples (Chromel-Constantan) with a precision of $\pm 0.05^\circ\text{C}$. The vapor temperature is measured by five thermocouples (T06, T07, T08, T09, and T10) in the test section. These thermocouples indicate the same temperatures (T_{sat}) during the condensation of HFC134a, in contrast to the condensation of HFC23/HFC134a, where the vapor temperature decreases from the inlet to the outlet of the test section. The temperatures indicated by the five thermocouples are interpolated in order to obtain the vapor temperature in the neighborhood of each row.

In this study, commercial tubes (Wieland-Werke AG) are used, having a wall thickness of about 1 mm. An indirect Wilson plot method which measures the vapor-side heat transfer coefficient without measuring the wall temperature is employed.

From the measured water temperatures in the mixing chambers at the inlet and the outlet of each tube and from the measured vapor temperature in the neighborhood of each row, the overall HTC is calculated as follows:

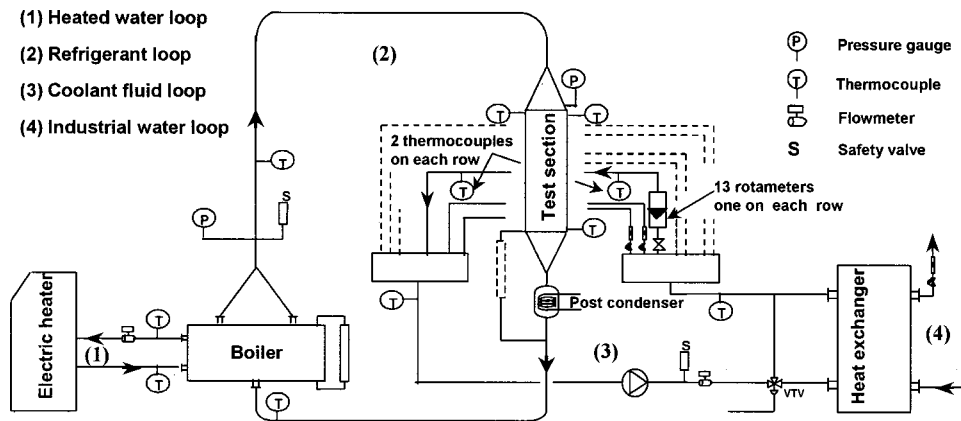


Fig. 2 Test rig

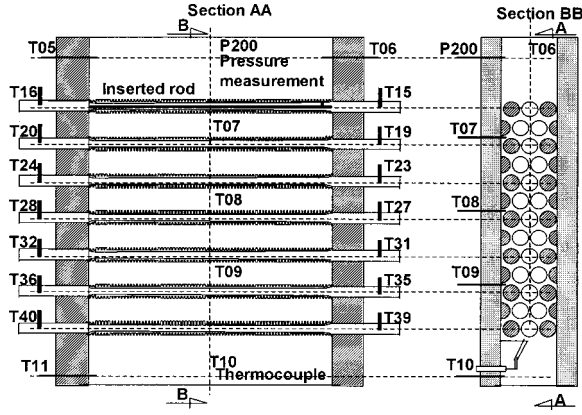


Fig. 3 Test section

Table 1 Tube dimensions (mm). See nomenclature for definitions. (The uncited dimensions are proprietary.)

Tube	D_r	D_e	D_i	p	h	t
smooth	16.8	16.8	14.2	---	---	---
K11	16	18.9	14	2.31	1.45	0.38
K19	16	18.9	14	1.34	1.45	0.33
K26	15.8	18.8	14	0.97	1.5	0.25
K32	16.2	18.8	14	0.82	1.3	0.2
K40	16.3	18.9	14.4	0.635	1.3	0.16
Gewa C+	17	---	14	---	---	---

$$U = \frac{\dot{m}_c C_{p,c}}{\pi D_r L_{\text{tube}}} \ln \left(\frac{T_{v,j} - T_{c,j,\text{in}}}{T_{v,j} - T_{c,j,\text{out}}} \right) \quad (1)$$

where j refers to the row number, c to the cooling water, v to the vapor, *in* and *out* to the cooling water input and output respectively. The reference area is that outside a bare tube, D_r being either the external diameter of a smooth tube or the diameter at the fin root for enhanced tubes.

The vapor-side HTC, α_e , is calculated via the following relation:

$$\frac{1}{\alpha_e} = \frac{1}{U} - \frac{1}{\alpha_i} \frac{D_r}{D_i} - \frac{D_r}{2\lambda_w} \ln \left(\frac{D_r}{D_i} \right) \quad (2)$$

α_i is the inner heat transfer coefficient determined with the Gnielinski correlation (Gnielinski [25]):

$$\text{Nu}_G = \frac{(f/2)(\text{Re}_c - 1000)\text{Pr}_c}{1 + 12.7(f/2)^{1/2}(\text{Pr}_c^{2/3} - 1)} \quad (3)$$

where f is the friction factor determined from the following expression:

$$f = (1.58 \ln(\text{Re}_c) - 3.28)^{-2} \quad (4)$$

Re_c is the hydraulic Reynolds given by:

$$\text{Re}_c = \frac{\rho_c \dot{V}_c D_h}{\mu_c} \quad (4\text{-bis})$$

The Gnielinski correlation has been chosen because it has a wide range of applicability, $2300 < \text{Re}_c < 5 \cdot 10^6$ and $0.5 < \text{Pr}_c < 2000$. Thus, it covers both the transition and the turbulent flow regimes. In our case, the Reynolds number was varied between 2,400 and 12,000.

The inner HTC α_i is expressed as:

Table 2 B values

Tube	Gewa C+	K40	K32	K26	K19	K11
B	1.07	1.19	0.99	0.98	1.08	0.92

$$\alpha_i = B \cdot \text{Nu}_G \cdot \frac{\lambda_c}{D_h} \quad (5)$$

where the coefficient B is determined by the Wilson plot procedure (Wilson [26]). To determine the B coefficient a specific loop was built with a water/water countercurrent double pipe heat exchanger. The inner tube is the same as used in the condensation experiments. To enhance the accuracy on the α_i value, the outer HTC in this specific loop was maintained to a high value. The uncertainty δB was determined using Moffat's method [27]. Table 2 gives the B values for all tubes tested.

The relative uncertainty of the vapor-side HTC is strongly depending on the experimental conditions. For example, for condensation on the first row the uncertainties are less than 20 percent, 17 percent, 21 percent, 17 percent, 14 percent, and 15 percent for the K11, K19, K26, K32, K40, and Gewa C+, respectively. For the whole bundle, the uncertainties are reported on the figures. Details of the uncertainty calculations are given in the appendix.

Experimental Results

Pure Fluid (HFC 134a)

Single Tube. Figure 4 shows the evolution of the HTC of the first row with temperature difference ΔT , during condensation of pure HFC134a on all tubes tested and on a smooth tube (Belghazi et al. [24]). It can be seen that K32 has the best performance compared to the other trapezoidal fin tubes. A fin spacing of about 0.6 mm is then an optimum in order to have the best heat transfer coefficient during condensation of HFC134a. The notched fin tube presents a better HTC than the K32 tube, because notches located at the middle of the fin height enhance surface tension effects at the fin tip. The film condensate is thinner and heat transfer performances are better.

To predict the Gewa C+ HTC a theoretical model based on the Nusselt approach but taking the surface tension into account, has been developed.

Tube Bundle. Figure 5 shows the evolution of the heat transfer coefficient along the bundle. It can be seen that the inundation effect (impinging of deep rows by condensate flowing from upper rows) is important for Gewa C+ tubes in contrast to trapezoidal fin tubes (Signe, [28]) where the deterioration of the HTC is not important. It is also noticed that the higher the vapor mass velocity G , the greater the Gewa C+ HTC deterioration in the tube

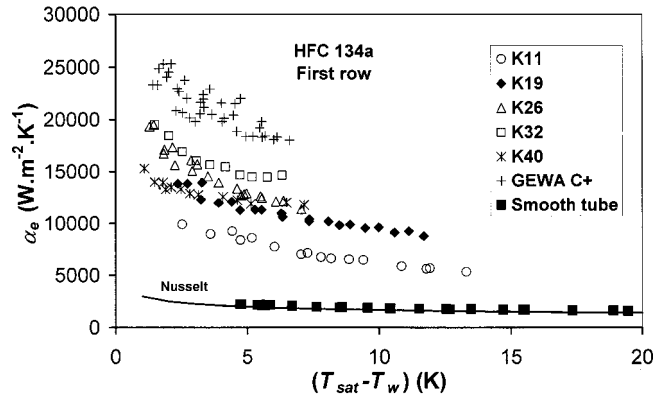


Fig. 4 Heat transfer coefficient of the first row during condensation of HFC134a

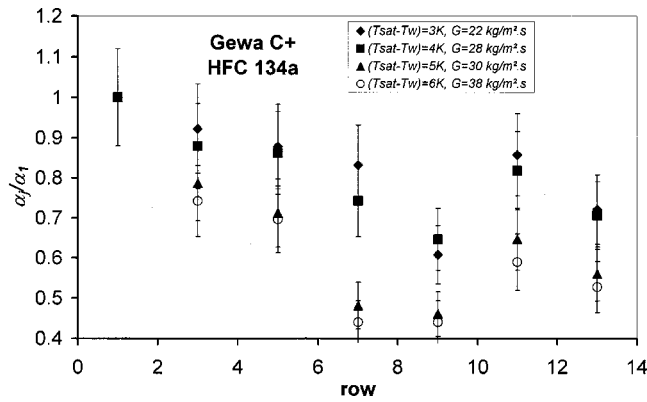


Fig. 5 Evolution of the Gewa C+ HTC along the bundle during condensation of HFC 134a

bundle, in contrast to the integral fin tubes where the deterioration of the HTC is more important when G decreases (Belghazi, [29]). Indeed, the Gewa C+ has low notched fins and retains condensate formed on the upper rows. Then, even if the vapor mass velocity increases, the inundation effect controls the heat transfer because the condensate flow increases also.

Mixtures

Single Tube. Figure 6 shows the evolution of the HTC during condensation of two mixtures (3 percent and 6 percent HFC23) of HFC23/HFC134a on K19 and Gewa C+ tubes. A deterioration of the mixture HTC is noted due to the mass transfer induced by the more volatile component (HFC23) which accumulates in the liquid-vapor interface and constitutes a diffusion layer which acts as a thermal resistance. Such deterioration has been also observed by Hijikata and Hemino [22], who measured the vapor-side HTC during condensation of R113 and several compositions of the mixture R113/R114.

Contrary to the case of the pure fluid it can be seen from Fig. 6 that the Gewa C+ has a HTC comparable to that of the K19 tube. Indeed, as the Gewa C+ tube has low fins compared to the other fin tubes, its fins are flooded by the diffusion layer (Fig. 7), and performance is poorer. For 6 percent HFC 23 and for low ΔT^* s, where the diffusion layer controls the heat transfer, the K19 and Gewa C+ HTC values tend to the smooth tube HTC values, since the diffusion layer is very thick and screens the fins. The finned tube is seen as a smooth tube.

Tube Bundle. During condensation of mixture outside the Gewa C+ bundle the HTC may increase or decrease from the top to the bottom of the tube bank, depending on the heat flux (Fig. 8).

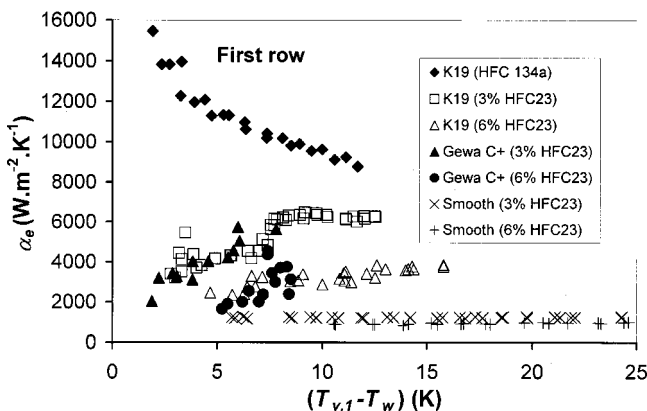


Fig. 6 Evolution of mixture HTC on Gewa C+ and K19 tubes

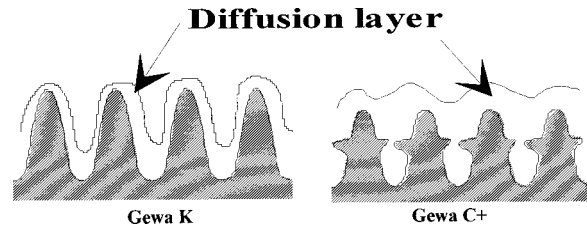


Fig. 7 Flooding of fins by the gaseous diffusion layer

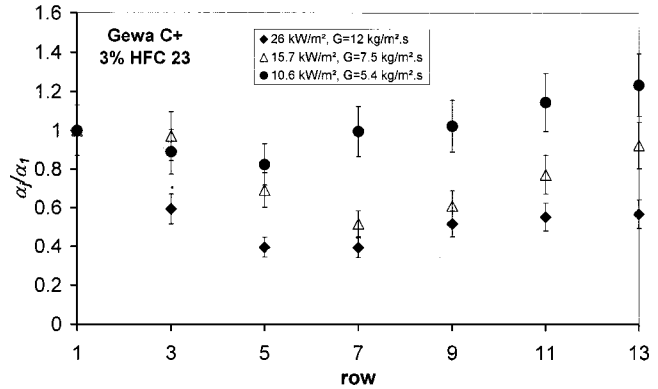


Fig. 8 Evolution of the ratio α_f/α_1 as a function of the row number

Such effects have already been observed by Signe [28] who noted that the HTC on a bundle of smooth tubes increases throughout the bundle. This effect was explained by the fact that the condensate formed on upper rows disturbs the diffusion layer, which gives an amelioration of the heat transfer.

Theoretical Model

As shown in Fig. 9, the Beatty and Katz model [1] underestimates the HTC of the Gewa C+ tube, because it neglects the surface tension effects which are enhanced by notches located at the fin flanks (Fig. 11). To develop a model predicting the HTC on the Gewa C+ tube, the tube circumference is divided into a flooded and an unflooded part.

The flooded part located at the bottom of the tube is referred to as an area submerged completely by the condensate because of capillary retention. It is assumed that there is no heat transfer in this part of the tube. The retention angle Φ (Fig. 10) is calculated by the Rudy and Webb equation [30]:

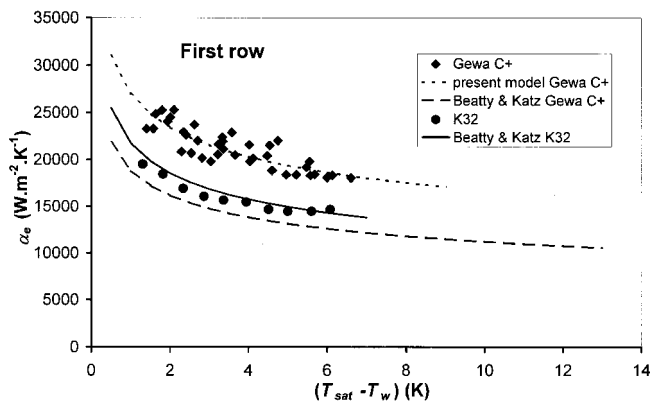


Fig. 9 Experimental and predicted HTC during condensation of HFC 134a on Gewa C+ and K32 tubes

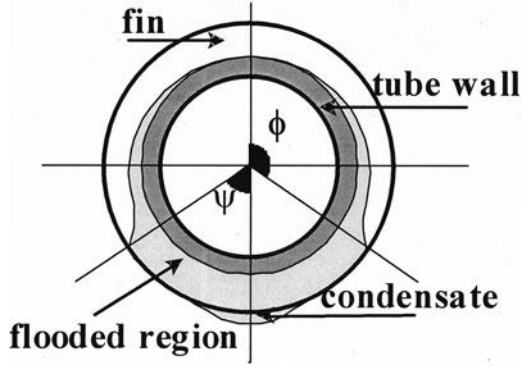


Fig. 10 Retention angle

$$\Phi = \cos^{-1} \left(\frac{4\sigma}{\rho_l g b D_e} - 1 \right)$$

The unflooded region is divided into four regions:

- region I: referred as the upper part of the fin, located above the notches
- region II: fin area beneath notches
- region III: fin area located between notches
- region IV: the interfin channel

It is assumed that the condensate is drained by surface tension in regions I and III, and by gravity in regions II and IV.

The model is based on the Nusselt expressions for condensation on a vertical plate (Eq. (7)), and on horizontal smooth tubes (Eq. (8))

$$\alpha_{\text{plate}} = 0.943 \left(\frac{\lambda_l^3 \rho_l (\rho_l - \rho_v) g \Delta h_v}{\mu_l (T_{\text{sat}} - T_w) L} \right)^{1/4} \quad (7)$$

$$\alpha_{\text{tube}} = 0.728 \left(\frac{\lambda_l^3 \rho_l (\rho_l - \rho_v) g \Delta h_v}{\mu_l (T_{\text{sat}} - T_w) D} \right)^{1/4} \quad (8)$$

where L and D are plate length and tube diameter, respectively.

For regions I and III where only surface tension forces drain condensate, Nusselt's expression (Eq. (7)) is modified by replacing $\rho_l g$, which is a gravity volume force, by an equivalent in terms of surface tension.

Generally the condensation of a fluid having a liquid-vapor interface radius (see Fig. 12) which varies along the wall, induces a pressure variation along that interface. An expression for this was given by (Gregorig, [7]):

$$\frac{dP_l}{ds} = \frac{d(\sigma/r)}{ds} \quad (9)$$

In term of a volume force Eq. (9) can be written:

$$dF_\sigma = \sigma \frac{d(1/r)}{ds} dV \quad (10)$$

where dV is a condensate volume control.

For a condensate film surface having two different radii r_t and r_b as shown in Fig. 12, the curvature derivative can be written as:

$$\frac{d(1/r)}{ds} \approx \frac{1}{h} \left(\frac{1}{r_b} - \frac{1}{r_t} \right) \quad (11)$$

where h is the fin height.

This nevertheless represents a strong assumption, which will be justified a posteriori.

Combining Eq. (10) and (11) gives:

$$\frac{dF_\sigma}{dV} \approx \frac{\sigma}{h} \left(\frac{1}{r_b} - \frac{1}{r_t} \right) \quad (12)$$

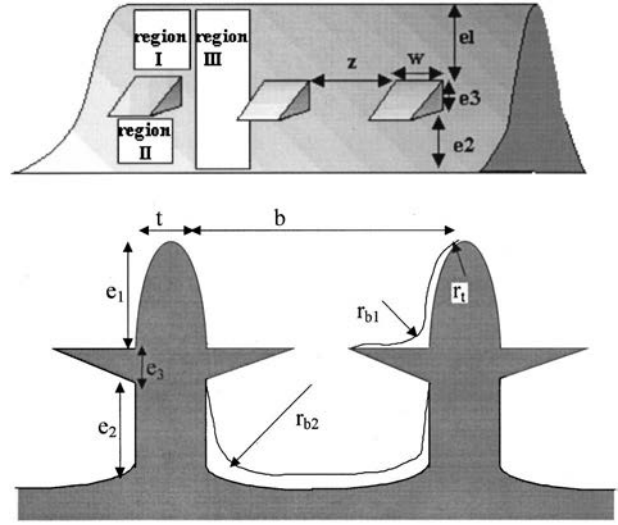


Fig. 11 The shape of the Gewa C+ tube. Definitions of parameters used

The Gewa C+ HTC, calculated with reference to the surface of tube having D_r as a diameter, is a function of the HTCs of regions I, II, III, and IV and is given by:

$$\alpha_p A_r = \eta (\alpha_I A_I + \alpha_{II} A_{II} + \alpha_{III} A_{III}) + \alpha_{IV} A_{IV} \quad (13)$$

where η is the fin efficiency, given by:

$$\eta = \frac{\tanh(mh)}{mh} \quad (14)$$

with

$$m = \left(\frac{2\alpha_p}{\lambda_w t} \right)^{1/2} \quad (15)$$

α_p being determined by an iterative procedure.

Parameters given in Eq. (13) are defined as follows:

$$A_I = 2 \frac{\Phi}{\pi} K w e_1 / p \quad (16)$$

$$A_{II} = 2 \frac{\Phi}{\pi} K w e_2 / p \quad (17)$$

$$A_{III} = 2 \frac{\Phi}{\pi} K z h / p = 2 \frac{\Phi}{\pi} K z (e_1 + e_2 + e_3) / p \quad (18)$$

$$A_{IV} = 2 \frac{\Phi}{\pi} K \pi D_r b / p \quad (19)$$

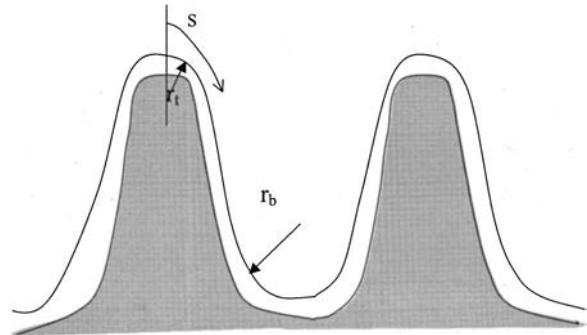


Fig. 12 Variation of the vapor interface radius

$$A_r = \pi D_r,$$

where K is the number of elemental parts of the fin (region I, II, III plus notches. Fig. 11) on one side of a fin flank and p is the fin pitch.

Assuming that (Fig. 11):

$$r_t = t/2; \quad r_{b1} = -b/4; \quad r_{b2} = -b/2$$

the acting force in the region I is given by:

$$\left. \frac{dF_\sigma}{dV} \right|_{\text{Region I}} = \frac{\sigma}{e_1} \left(\frac{1}{r_t} + \frac{1}{r_{b1}} \right) = \frac{\sigma}{e_1} \left(\frac{2}{t} + \frac{4}{b} \right) \quad (20)$$

Substituting $\rho_l g$ in Eq. (7) by Eq. (20) leads to:

$$\alpha_I = 0.943 \left(\frac{\lambda_l^3 (\rho_l - \rho_v) \Delta h_v}{\mu_l (T_{\text{sat}} - T_w) e_1} \right)^{1/4} \left(\frac{\sigma}{e_1} \left(\frac{2}{t} + \frac{4}{b} \right) \right)^{1/4} \quad (21)$$

In the same manner in region III:

$$\left. \frac{dF_\sigma}{dV} \right|_{\text{Region III}} = \frac{\sigma}{h} \left(\frac{1}{r_t} + \frac{1}{r_{b2}} \right) = \frac{2\sigma}{h} \left(\frac{1}{t} + \frac{1}{b} \right) \quad (22)$$

$$\alpha_{\text{III}} = 0.943 \left(\frac{\lambda_l^3 (\rho_l - \rho_v) \Delta h_v}{\mu_l (T_{\text{sat}} - T_w) h} \right)^{1/4} \left(\frac{2\sigma}{h} \left(\frac{1}{t} + \frac{1}{b} \right) \right)^{1/4}. \quad (23)$$

In region II, the condensate is drained by gravity and the HTC is given by:

$$\alpha_{\text{II}} = 0.943 \left(\frac{\lambda_l^3 \rho_l (\rho_l - \rho_v) g \Delta h_v}{\mu_l (T_{\text{sat}} - T_w) e_2} \right)^{1/4} \quad (24)$$

The HTC in the interfin channel is given using Eq. (8) by:

$$\alpha_{\text{channel}} = 0.728 \left(\frac{\lambda_l^3 \rho_l (\rho_l - \rho_v) g \Delta h_v}{\mu_l (T_{\text{sat}} - T_w) D_r} \right)^{1/4} \quad (25)$$

The condensate formed on fins is collected within the interfin channel, so that the actual HTC corresponding to the region IV is smaller than the one calculated by Eq. (25) since film condensate is thicker. To take this phenomenon into account another version of the Nusselt formula is used (Eq. (26)):

$$\alpha_{\text{IV}} = 1.51 \text{Re}_f^{-1/3} \left(\frac{\nu_l^2}{\lambda_l^3 g} \right)^{-1/3} \quad (26)$$

where

$$\text{Re}_f = 4 \frac{\Gamma}{\mu_l} \quad \text{and} \quad \Gamma = \Gamma_{\text{channel}} + \Gamma_{\text{fin}}$$

$$\Gamma_{\text{channel}} = \frac{\alpha_{\text{channel}} (T_{\text{sat}} - T_w) A_{\text{IV}}}{\Delta h_v} \quad (27)$$

$$\Gamma_{\text{fin}} = \eta \frac{(\alpha_I A_I + \alpha_{\text{II}} A_{\text{II}} + \alpha_{\text{III}} A_{\text{III}}) (T_{\text{sat}} - T_w)}{\Delta h_v} \quad (28)$$

Figure 9 shows that the present model predicts very accurately the Gewa C+ HTC, without adjusting any parameter. The deviation from experimental results is less than 10 percent.

Conclusion

The present investigation allows the following concluding remarks to be drawn:

- Experimental data for condensation of HFC134a on five commercially available copper integral fin tubes show an optimum fin spacing of about 0.6 mm.
- The Gewa C+ tube (notched tube) has been tested and gives an enhancement of about 30 percent compared to the best integral fin tubes (K32). Notches drawn on fin flanks enhance the surface tension effect. During condensation of HFC134a, the higher the vapor mass velocity, the greater the Gewa C+ HTC deterioration

in the tube bundle. However, from an industrial point of view, the usual ΔT is about 3K, and in this case the inundation effect is not significant.

• For the mixtures, experimental results show that, due to the zeotropic character of the mixture tested (HFC23/HFC134a), the HTC deteriorates dramatically. Contrary to the pure fluid case, the Gewa C+ tube gives no enhancement compared to the K19 tube.

• The model developed for a single Gewa C+ tube, takes into account surface tension effects, and predicts accurately the present experimental data.

• Work is currently in progress to develop a model, based on the condensation curve method, predicting heat transfer during condensation of binary mixtures outside a bundle of Gewa C+.

Acknowledgment

The authors acknowledge with thanks Wieland-Werk AG for their contribution to this work.

Nomenclature

A	= heat exchange surface area, m ²
A_r	= surface of a plain tube, m ²
b	= fin spacing, m
C_p	= heat capacity, J kg ⁻¹ K ⁻¹
D_0	= diameter of the metallic rod, m
D_e	= diameter at the fin tip, m
D_h	= hydraulic diameter, m
D_i	= inner diameter, m
D_r	= tube diameter at the fin root, m
e_1	= distance from fin tip to notch, m
e_2	= distance from notch to fin root, m
e_3	= thickness of a notch, m
f	= friction factor
F	= force, N
g	= gravity, m s ⁻²
G	= vapor mass velocity, kg m ⁻² s ⁻¹
h	= fin height, m
K	= number of elemental parts on fin's flank
L	= plate length, m
L_{tube}	= tube length, m
\dot{m}	= mass flow rate, kg s ⁻¹
p	= fin pitch, m
P	= pressure, Pa
\dot{Q}	= heat flow rate, W
r	= curvature radius, m
r_{b1}, r_{b2}, r_t	= curvature radii, m
s	= curvilinear coordinate, m
t	= fin thickness, m
T	= temperature, K
U	= overall heat transfer coefficient, W m ⁻² K ⁻¹
\dot{V}	= volumetric flow rate, m ³ s ⁻¹
w	= notch width, m
z	= space between notches, m

Greek

α_e	= vapor side HTC, W m ⁻² K ⁻¹
α_i	= inner HTC, W m ⁻² K ⁻¹
α_p	= predicted HTC, W m ⁻² K ⁻¹
ΔT	= $(T_{\text{sat}} - T_w)$ or $(T_{\text{vj}} - T_w)$, K
Δh_v	= latent heat, J kg ⁻¹
Γ	= condensate lineic mass flow rate, kg s ⁻¹ m ⁻¹
Φ	= flooding angle, rad
λ	= thermal conductivity, W m ⁻¹ K ⁻¹
μ	= dynamic viscosity, Pa s
ν	= kinematic viscosity, m ² s ⁻¹
ρ	= density, kg m ⁻³
σ	= surface tension, N m ⁻¹
η	= fin efficiency

Indices

- I, II, III, IV = region's index
 c = coolant
 e = external
 f = film condensate
 G = refers to Gnielinski
 i = internal
 in = water inlet
 j = row index
 l = liquid
 out = water outlet
 r = at fin root
 t = fin tip
 v = vapor
 w = wall
 σ = refers to surface tension

Dimensionless Numbers

- Nu = Nusselt number
 Pr = Prandtl number
 Re = Reynolds number

Appendix

The single sample uncertainty of external heat transfer coefficient, $\delta\alpha_e$, is written as:

$$\delta\alpha_e = \sqrt{\left(\frac{\partial\alpha_e}{\partial U} \delta U\right)^2 + \left(\frac{\partial\alpha_e}{\partial\alpha_i} \delta\alpha_i\right)^2} \quad (A-1)$$

where

$$\frac{\partial\alpha_e}{\partial U} = \frac{1}{U^2 \left\{ \frac{1}{U} - \frac{1}{\alpha_i} \frac{D_r}{D_i} - \frac{D_r}{2\lambda_w} \text{Ln} \left(\frac{D_r}{D_i} \right) \right\}^2} \quad (A-2)$$

and

$$\frac{\partial\alpha_e}{\partial\alpha_i} = - \frac{1}{\alpha_i^2 \left\{ \frac{1}{U} - \frac{1}{\alpha_i} \frac{D_r}{D_i} - \frac{D_r}{2\lambda_w} \text{Ln} \left(\frac{D_r}{D_i} \right) \right\}^2} \quad (A-3)$$

In the same way:

$$U = \frac{\dot{m}_c C_p}{\pi D_r} \text{Ln} \left(\frac{T_v - T_{c,in}}{T_v - T_{c,out}} \right) \quad (A-4)$$

$$\delta U = \sqrt{\left(\frac{\partial U}{\partial \dot{m}_c} \delta \dot{m}_c\right)^2 + \left(\frac{\partial U}{\partial T_v} \delta T_v\right)^2 + \left(\frac{\partial U}{\partial T_{c,out}} \delta T_{c,out}\right)^2 + \left(\frac{\partial U}{\partial T_{c,in}} \delta T_{c,in}\right)^2} \quad (A-5)$$

The flowmeter used has a precision of 0.5 percent, and the thermocouples have an uncertainty of 0.05 K.

$$\alpha_i = B \cdot \text{Nu}_G \frac{\lambda_c}{D_h} \quad (A-6)$$

$$\delta\alpha_i = \sqrt{\left(\frac{\partial\alpha_i}{\partial B} \delta B\right)^2 + \left(\frac{\partial\alpha_i}{\partial \text{Nu}_G} \delta \text{Nu}_G\right)^2} \quad (A-7)$$

Using Moffat's method [27] it was found that δB is equal to 0.1, 0.09, 0.04, 0.12, 0.03 and 0.05 for K11, K19, K26, K32, K40 and Gewa C+ respectively.

For each point δNu_G is calculated as follows:

$$\delta \text{Nu}_G = \frac{\partial \text{Nu}_G}{\partial \text{Re}} \delta \text{Re} \quad (A-8)$$

where Nu_G is given by equations (3) and (4).

$$\delta \text{Re} = \frac{4\rho_c}{\pi\mu_c(D_i + D_0)} \delta \dot{V}_c \quad (A-9)$$

Finally the maximum relative uncertainty of the external HTC $\delta\alpha_e/\alpha_e$ for the first row of the bundle is equal to 20 percent, 17 percent, 21 percent, 17 percent, 14 percent and 15 percent for the K11, K19, K26, K32, K40 and Gewa C+ respectively. For the bundle the uncertainties are reported on the figures 5 and 8.

References

- [1] Beatty, K. O., and Katz, D. L., 1948, "Condensation of Vapors on Outside of Finned Tubes," Chem. Eng. Prog., **44**, pp. 55–77.
- [2] Karkhu, V. A., and Borovkov, V. P., 1971, "Film Condensation of Vapor at Finely Finned Horizontal Tubes," Heat Transfer-Sov. Res., **3**(2), pp. 183–191.
- [3] Webb, R. L., Rudy, T. M., and Kedzierski, M. A., 1985, "Prediction of Condensation Coefficient on Horizontal Integral-Fin Tubes," ASME J. Heat Transfer, **107**, pp. 369–376.
- [4] Honda, H., and Nozu, S., 1987, "A Prediction Method for Heat Transfer During Film Condensation on Horizontal Low Integral-Fin Tubes," ASME J. Heat Transfer, **109**, pp. 218–225.
- [5] Adamek, T., and Webb, R. L., 1990, "Prediction of Film Condensation on Horizontal Integral-Fin Tubes," Int. J. Heat Mass Transf., **33**(8), pp. 1721–1735.
- [6] Rose, J. W., 1994, "An Approximation Equation for the Vapor-Side Heat-

- Transfer Coefficient for Condensation on Low-Finned Tubes," Int. J. Heat Mass Transf., **37**, pp. 865–875.
- [7] Sreepathi, L. K., Bapat, S. L., and Sukhatme, S. P., 1996, "Heat Transfer During Film Condensation of R-123 Vapor on Horizontal Integral-Fin Tubes," Journal of Enhanced Heat Transfer, **3**(2), pp. 147–164.
- [8] Gregorig, R., 1954, "Film Condensation on Finely Rippled Surfaces with Consideration of Surface Tension," Z. Angew. Math. Phys., **5**, pp. 36–49.
- [9] Adamek, T., 1981, "Bestimmung der Kondensations-grossen auf Feingewellten Oberflachen zur Auslegung Optimaler Wandprofile," Waerme- Stoffuebertrag., **15**, pp. 255–270.
- [10] Zhu, H.-R., and Honda, H., 1993, "Optimization of Fin Geometry of a Horizontal Low-Finned Condenser Tube," Heat Transfer-Jpn. Res., **22**(4), pp. 372–386.
- [11] Honda, H., and Kim, K., 1995, "Effect of Fin Geometry on the Condensation Heat Transfer Performance of a Bundle of Horizontal Low-Finned Tubes," J. Enhanced Heat Transfer, **2**(1–2), pp. 139–147.
- [12] Honda, H., and Makishi, O., 1995, "Effect of Circumferential Rib on Film Condensation on a Horizontal Two-Dimensional Fin Tube," J. Enhanced Heat Transfer, **2**(4), pp. 307–315.
- [13] Webb, R. L., Keswani, S. T., and Rudy, T. M., 1982, "Investigation of Surface Tension and Gravity Effects in Film Condensation," Proc. Int. Heat Transfer Conf., Washington, **5**, pp. 175–180.
- [14] Honda, H., Uchima, B., Nozu, S., Nakada, H., and Torigoe, E., 1991, "Film Condensation of R-113 on In-Line Bundles of Horizontal Finned Tubes," ASME J. Heat Transfer, **113**(2), pp. 479–486.
- [15] Honda, H., Uchima, B., Nozu, S., Torigoe, E., and Imai, S., 1992, "Film Condensation of R-113 on Staggered Bundles of Horizontal Finned Tubes," ASME J. Heat Transfer, **114**(2), pp. 442–449.
- [16] Wang, S. P., Hijikata, K., and Deng, S. J., 1990, "Experimental Study on Condensation Heat Transfer Enhancement by Various Kinds of Integral Finned Tubes," Condensers and Condensation, Proc. 2nd Int. Symp., pp. xv–xxiii.
- [17] Webb, R. L., and Murawski, C. G., 1990, "Row Effect for R-11 Condensation on Enhanced Tubes," ASME J. Heat Transfer, **112**, pp. 768–775.
- [18] Blanc, P., Bontemps, A., and Marvillet, C., 1994, "Condensation Heat Transfer of HCFC22 and HFC134a Outside a Bundle of Horizontal low Finned Tubes," Proc. Symp. CFC's, The Day After, Padova, Italy, pp. 635–642.
- [19] Honda, H., Takamatsu, H., Takada, N., and Yamasaki, T., 1995, "Condensation of HFC 134a and HFC 123 in a Staggered Bundle of Horizontal Finned Tubes," Proc. Eurotherm No. 47, Heat Transfer in Condensation, pp. 110–115, Paris.
- [20] Cheng, W. Y., and Wang, C., 1994, "Condensation of R-134a on Enhanced Tubes," ASHRAE Trans., **10**(1), pp. 809–819.
- [21] Agrawal, K. N., Moharty, P., Kumar, R., and Varma, H. K., 1999, "Enhancement of Heat Transfer Rates During Condensation of Refrigerants Over Horizontal Finned Tubes," Proc. Symp. Two Phase Flow Modelling and Experimentation, **1**, pp. 505–510.
- [22] Hijikata, K., and Himeno, N., 1990, "Condensation of Azeotropic and Non-azeotropic Binary Vapor Mixtures," Annu. Rev. Heat Transfer, **3**, Chap. 2, pp. 39–83.

- [23] Honda, H., Takuma, M., and Takada, N., 1999, "Condensation of Downward-Flowing Zeotropic Mixture HFC-123/HFC-134a on a Staggered Bundle of Horizontal Low-Finned Tubes," *ASME J. Heat Transfer*, **121**, pp. 405–412.
- [24] Belghazi, M., Bontemps, A., Signe, J. C., and Marillet, C., 2001, "Condensation Heat Transfer of a Pure Fluid and Binary Mixture outside a Bundle of Smooth Horizontal Tubes. Comparison of Experimental Results and a Classical Model," *Int. J. Refrig.*, **24**(8), pp. 841–855.
- [25] Gnielinski, V., 1976, "New Equation for Heat and Mass Transfer in Turbulent Pipe and Channel Flow," *Int. Chem. Eng.*, **16**(2), pp. 359–368.
- [26] Wilson, E. E., 1915, "A Basis for Rational Design of Heat Transfer Apparatus," *Trans. ASME*, **37**, pp. 47–70.
- [27] Moffat, R. J., 1988, "Describing the Uncertainties in Experimental Results," *Exp. Therm. Fluid Sci.*, **1**, pp. 3–17.
- [28] Signe, J. C., 1999, "Condensation de Mélanges Non Azéotropes de Fluides Frigorigènes à l'Extérieur d'un Faisceau de Tubes Horizontaux," Ph.D. thesis, Université Joseph Fourier, Grenoble, France.
- [29] Belghazi, M., 2001, "Condensation d'un fluide pur et de mélanges zéotropes à l'extérieur d'un faisceau de tubes à surface améliorée," Ph.D. thesis, Université Joseph Fourier, Grenoble, France.
- [30] Rudy, T. M., and Webb, R. L., 1985, "An Analytical Model to Predict Condensate Retention on Horizontal Integral-Fin Tubes," *ASME J. Heat Transfer*, **107**, pp. 361–368.